A Technology-Based Compact Model for Predictive Deep-Submicron MOSFET Modeling and Characterization

Xing Zhou*, Siau Ben Chiah* and Khee Yong Lim**

*School of Electrical & Electronic Engineering, Nanyang Technological University
Nanyang Avenue, Singapore 639798, exzhou@ntu.edu.sg
**Chartered Semiconductor Manufacturing Ltd, 60 Woodlands Industrial Park D, St 2, Singapore 738406

ABSTRACT

This paper presents new development results of our compact model (Xsim) for deep-submicron MOSFETs. Although a threshold-voltage-based and source-referenced regional model, Xsim meets the basic requirements of continuity (to third-order derivatives), scalability (entire geometry range), and symmetry, with a single-piece unified equation that approaches the ideal long/wide-channel expression. Model calibration requires minimum measurement data with one-iteration parameter extraction, which can be extrapolated to predicting characteristics of extremely-scaled devices with severe threshold voltage roll-off, a regime in which most common models do not (or cannot) model.

Keywords: Compact model, deep-submicron MOSFETs, scalability, symmetry, technology development.

1 INTRODUCTION

Compact models (CMs) for circuit simulation have been at the heart of CAD tools for circuit design over the past decades, and are playing an ever increasingly important role in the very-deep-submicron (VDSM) era. The current practice is to use the industry standard model, BSIM [1], on the golden die of a given technology by fitting a large number of parameters on a large set of measured electrical data. The model is optimized at the designed feature geometry, and not meant to be extrapolated outside the fitted range. To meet the increasing demand in accurate and continuous (in higher-order derivatives) modeling in the weak-inversion regime, "surface-potential-based" (as opposed to "threshold-voltage-based") approach is becoming popular [2]–[4]. Another basic requirement for MOS CM is source–drain symmetry, for which a "bulk-referenced" (as opposed to "source-referenced") model is generally favored. However, unlike in the "old" (micron) technology generations, in the VDSM era, geometry dependence (scalability) of a CM becomes extremely important due to strong lateral nonuniformity (such as halo) in a MOSFET since even a small gate-length variation is having a similar effect as due to drain-source voltage variation. Single-transistor-based models that are based on solving the surface potential (physically, iteratively, or approximately) would need empirical relations (at best, with simplified assumptions) to account for geometry effects. Moreover, a bulk-referenced model does not necessarily guarantee symmetry if lateral-field mobility and velocity saturation are not handled correctly [5]. Finally, if a CM's fitting parameters (no matter how many) have to be obtained through global optimization without physical relation to process variations, it may fit one transistor perfectly but may lose predictability for other transistors of the given technology.

The essence of MOS compact modeling is essentially a tradeoff among accuracy, continuity, symmetry, scalability, predictability, and efficiency. The ability of a CM in predicting electrical characteristics with accuracy in the second-/third-order derivatives from long/wide-channel down to the threshold-voltage (V_t) roll-off regime is a major challenge, which is important for capturing geometry variations due to process fluctuations, for predicting new technologies, as well as for analog circuit design.

This paper presents our approach to CM development (named Xsim [6]–[11]), which has a small number of (dc) fitting parameters that requires a *one-iteration* extraction procedure using minimum measurement data, and demonstrates its predictive capability in modeling short-channel effects (SCEs) in the V_t roll-off regime, accurate higher-order derivatives, as well as symmetry.

2 MODEL OVERVIEW

Xsim is a single-piece, source-referenced, threshold-voltage-based, regional model developed by adding SCEs to the well-known long-channel equations with physical modeling in the respective strong/weak-inversion and linear/saturation regions joined by smoothing functions. The main features include: physical modeling of V_t [6]–[8] by technology characterization (fitting V_t–L data at corner bias) that includes charge sharing and barrier lowering from quasi-2D solution, together with *halo centroid* modeled by two Gaussian lateral nonuniform doping profiles and LDD lateral diffusion for effective channel length (L_{eff}) extraction; semi-empirical vertical-field mobility (μ_0) modeling and new velocity–field and effective field (E_{eff}) formulations for lateral-field and bulk-charge (A_b) effects; bias-dependent series resistance (R_{sd}) modeling; channel-length modulation (CLM) formulated with energy-balance equations for *overshoot* effect with a <u>single</u> fitting parameter (ξ) in the *effective Early voltage* (V_{Aeff}) for all length/bias conditions [9]; a novel analytical "drift + diffusion" formulation with smooth weak/strong-inversion transition for all length/bias with one fitting parameter (V_{off}) [10]; and poly-gate depletion effect. Our new developments on the narrow-width effects [11] include a unified V_t model to account for the fringing capacitance, surface-potential lowering, and effective doping for the pile-up charge in shallow-trench isolated structures, as well as width-dependent phonon mobility correlation and dog-bone geometry for the external series resistance.

The complete I_{ds} equation [11] is extremely clean and compact with each internal term representing the respective physics, which also resembles (and approaches) the ideal long-channel equation (in the long-channel limit):

$$I_{ds} = I_{deff} / \left[1 + \left(R_{sd} I_{deff}\right)/V_{deff}\right] \quad (1)$$

$$I_{deff} = \left[1 + \left(V_{ds} - V_{deff}\right)/V_{Aeff}\right] I_{ds0} \quad (2)$$

$$I_{ds0} = \beta_n V_{ge} = \mu_{eff} C_{ox} \left(W_{eff} / L_{eff}\right)\left(V_{gg} + V_{gd}\right) \quad (3)$$

where V_{deff} (BSIM smoothing function [1]) links linear (V_{ds}) and saturation (V_{dsat}) regions (with a smoothing parameter, δ_s). V_{ge} (effective gate/drain-voltage product) represents the sum of drift (V_{gg}) and diffusion (V_{gd}) components, including a bulk-charge term $V_{de} = (1 - A_b V_{deff}/2V_{geff})V_{deff}$, linked by V_{geff} (BSIM interpolation function [1]), which approaches $V_{ge} \to V_{gg} \to V_{drift} = (V_{gs}-V_t)[1 - A_b V_{deff}/2(V_{gs}-V_t)]V_{deff}$ and $V_{ge} \to V_{gd} \to V_{diff} = v_{th}^2(C_d/C_{ox})e^{(V_{gs}-V_t-V_{off})/nv_{th}}(1 - e^{-V_{ds}/v_{th}})$ in strong and weak inversions, respectively, with the correct asymptotes and smooth transitions. The effective Early voltage (V_{Aeff}) incorporates all length/bias dependencies of CLM/velocity overshoot effects and expressed in the familiar form of the "pinch-off" model. All fitting parameters are extracted at the corner conditions at which they are defined in a one-iteration procedure.

3 RESULTS AND DISCUSSION

Figs. 1~3 show Xsim results (in comparison with BSIM3v3) for three devices from the 0.18-μm technology, where Xsim used only the V_t–L data (in Fig. 5) plus 5 I_{ds}–V_{gs} data at low/high V_{ds} (zero V_{bs}) for the 0.16/10μm and at low-V_{ds}/high-V_{bs} for the 10μm devices, as well as I_{ds}–V_{ds} for each device; whereas BSIM used all available I_{ds}–V_{gs} and I_{ds}–V_{ds} data (all 0.18~10μm devices). Xsim's approach is to "bracket" the optimized device (0.18μm), thus, geometry variation (down to 0.16μm) can be accurately modeled. Direct extrapolation to 0.15μm (no data used), as shown in Figs. 1,2,3(*c*), demonstrates the physics built into the model. The discrepancy is mainly due to V_t not being fitted, which can be improved if calibrated down to 0.15μm (shown in Fig. 5, cross-dotted); while a full re-calibration for the 0.15μm device (using three I_{ds} data) can well model the MOSFET in deep V_t roll-off (see Fig. 4). The g_{ds} and V_{Aeff} calibration uses g_{ds}'' data to determine the optimized δ_s value (related to the V_{ds} location of linear/saturation transition determined by the peak of g_{ds}''), and optimizes v_{sat} on I_{ds} data and ξ on g_{ds} data for each device. This assigns "physical" meanings (related to g_{ds}'') to the smoothing function parameter δ_s and the v_{sat} and V_{Aeff} interpretations (see Figs. 6 and 7), which are empirically modeled by length-dependent functions. The novel "$I_{drift} + I_{diff}$" formulation provides smooth and physical modeling in weak inversion, as shown in Fig. 8. Smooth derivatives are evidenced in g_m/I_{ds} and g_{ds} vs. log(I_{ds}) characteristics, as shown in Fig. 9. Source–drain symmetry is shown in Fig. 10, with smooth first/second derivatives at zero V_{ds}, which is attributed to the correct physical modeling of g_{ds}' for all geometry/bias conditions.

4 CONCLUSION

The Xsim model has demonstrated predictive capability for modeling VDSM technologies, as the model is scalable and technology-based, with minimum parameter and measurement data requirements. As SOI and double-gate technologies are entering the mainstream, source-referencing will find its advantage over bulk-referenced models. Although still under development/improvement, this regional/source-referenced/V_t-based model has already demonstrated smooth transitions and symmetry (as compared to popular surface-potential-based models), and especially its validity and predictability in large geometry range. It will have significant impact on modeling VDSM MOSFETs for circuit simulation that combines the essential features of model accuracy, continuity, scalability, predictability, symmetry, and simplicity.

REFERENCES

[1] Y. Cheng, *et al.*, "BSIM3v3 Manual," UC Berkeley, 1997.

[2] G. Gildenblat and T.-L. Chen, *Proc. MSM2002*, pp. 657–661, 2002.

[3] M. Miura-Mattausch, *et al.*, *Proc. MSM2002*, pp. 678–681, 2002.

[4] http://www.semiconductors.philips.com/Philips_Models/

[5] Y. Tsividis, "Operation and Modeling of the MOS Transistor," McGraw-Hill, 2nd ed., pp. 179–181, 1999.

[6] X. Zhou and K. Y. Lim, *IEEE Trans. Electron Devices*, vol. 48, pp. 887–896, 2001.

[7] X. Zhou, S. B. Chiah, K. Y. Lim, Y. Wang, X. Yu, S. Chwa, A. See, and L. Chan, *Proc. ICSICT-2001*, Shanghai, 2001, pp. 855–860.

[8] X. Zhou, Proc. MSM2002, pp. 710–714, 2002.

[9] K. Y. Lim and X. Zhou, *Microelectronics Rel.*, vol. 42, pp. 1857–1864, 2002.

[10] K. Y. Lim and X. Zhou, *IEEE Trans. Electron Devices*, vol. 49, pp. 196–199, 2001; also: S. B. Chiah, X. Zhou, K. Y. Lim, submitted for publication.

[11] S. B. Chiah, X. Zhou, and K. Y. Lim, to appear in *Proc. MSM2003*, San Francisco, 2003.

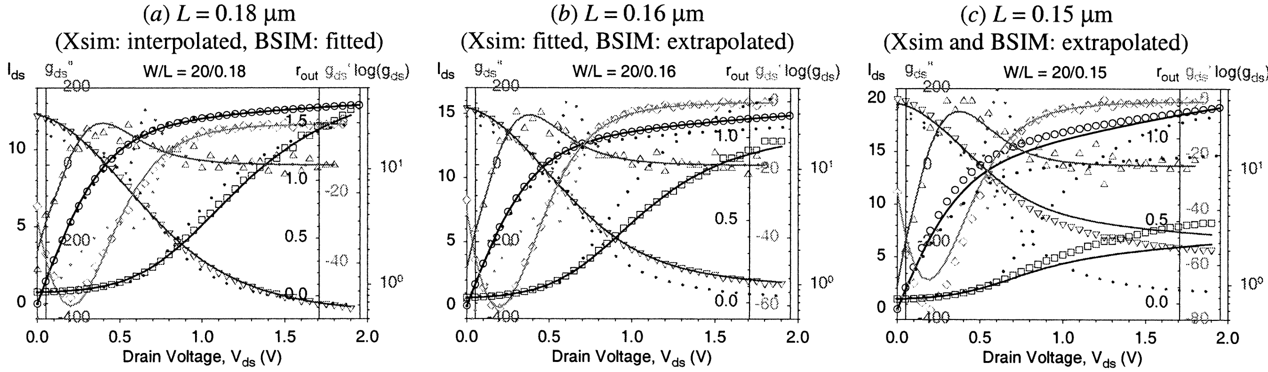

Figure 1: Measured (*symbols*) and modeled (Xsim: *solid lines*, BSIM: *dotted lines*) strong-inversion drain characteristics (V_{gs} = 1.8 V, V_{bs} = 0) of I_{ds} (○, mA), log(g_{ds}) (▽, mS), r_{out} (□, kΩ), g_{ds}' (◇, mS/V), and g_{ds}'' (△, mS/V^2) for the three gate-length devices.

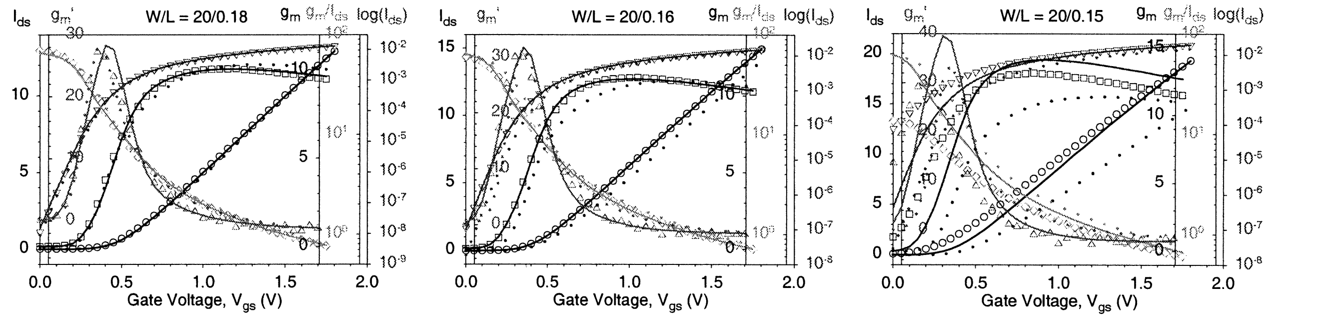

Figure 2: Measured (*symbols*) and modeled (Xsim: *solid lines*, BSIM: *dotted lines*) saturation gate characteristics (V_{ds} = 1.98 V, V_{bs} = 0) of I_{ds} (○, mA), log(I_{ds}) (▽, A), g_{ms} (□, mS), log(g_{ms}/I_{ds}) (◇, 1/V), and g_{ms}' (△, mS/V) for the three gate-length devices.

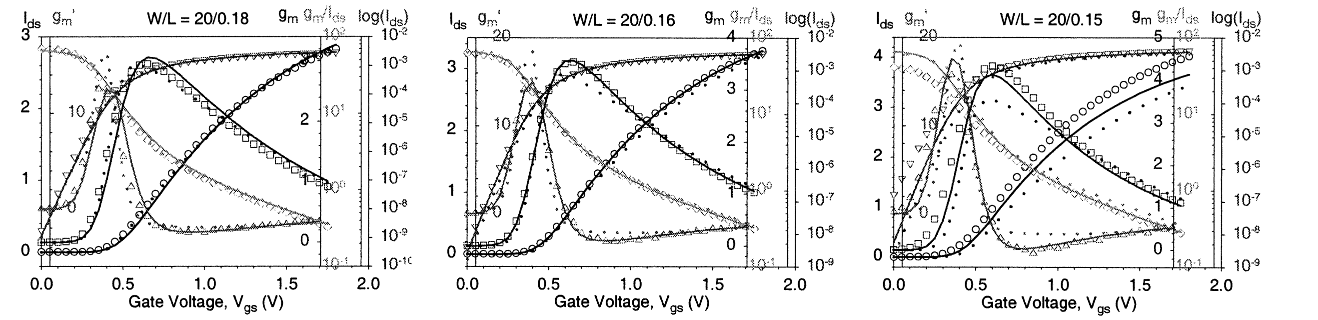

Figure 3: Measured (*symbols*) and modeled (Xsim: *solid lines*, BSIM: *dotted lines*) linear gate characteristics (V_{ds} = 0.1 V, V_{bs} = 0) of I_{ds} (○, mA), log(I_{ds}) (▽, A), g_{m0} (□, mS), log(g_{m0}/I_{ds}) (◇, 1/V), and g_{m0}' (△, mS/V) for the three gate-length devices.

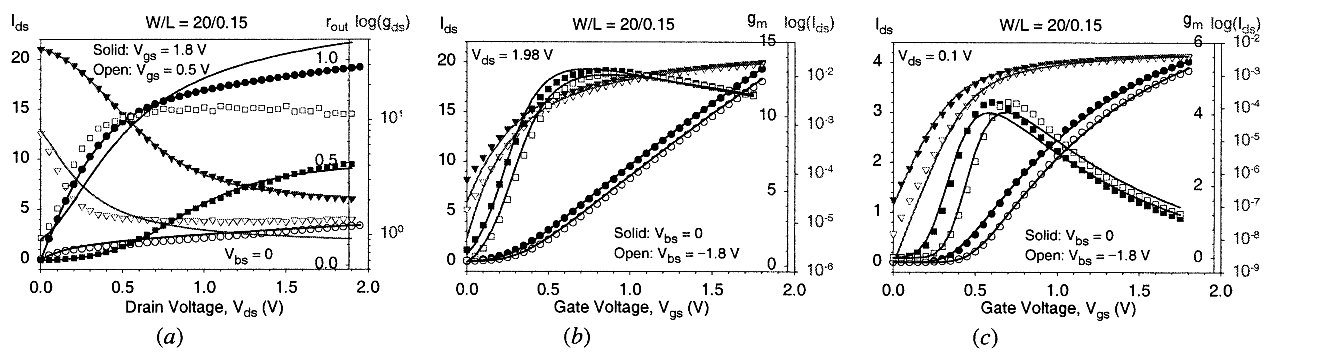

Figure 4: Measured (*symbols*) and modeled (*lines*) current/conductance characteristics of the 0.15-µm device for (*a*) output characteristics: I_{ds} (○, mA), log(g_{ds}) (▽, mS), r_{out} (□, kΩ) at high (*solid symbols*) and low (*open symbols*) V_{gs}, (*b*) saturation and (*c*) linear transfer characteristics: I_{ds} (○, mA), log(I_{ds}) (▽, A), g_m (□, mS) at low (*solid symbols*) and high (*open symbols*) V_{bs}. The *solid lines* are Xsim model with a re-calibration of the V_t model including the 0.15-µm V_t data (dotted lines in Fig. 5) and the I_{ds} model using the three I_{ds} data shown in solid circles plus I_{ds}–V_{gs} at V_{ds} = 0.1 V, V_{bs} = −1.8 V for bulk-bias calibration, which demonstrates Xsim's capability of modeling devices with severe SCEs ($V_{tsat} \approx 0$).

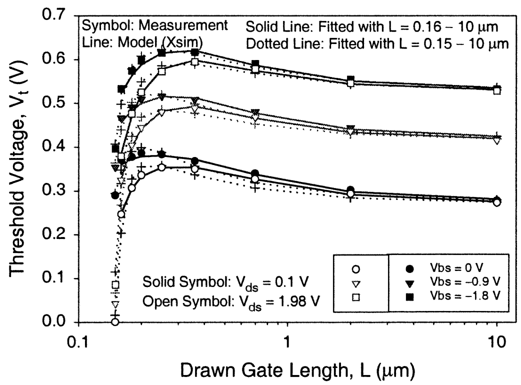

Figure 5: Measured (*symbols*) and modeled (*lines*) threshold-voltage (constant-current definition) characteristics at the corner V_{bs} and V_{ds}. *Solid lines* are fitted with the hard corner 0.16-μm (used in Figs. 1~3, solid lines), and *dotted lines* are for the hard corner 0.15-μm (used in Fig. 4).

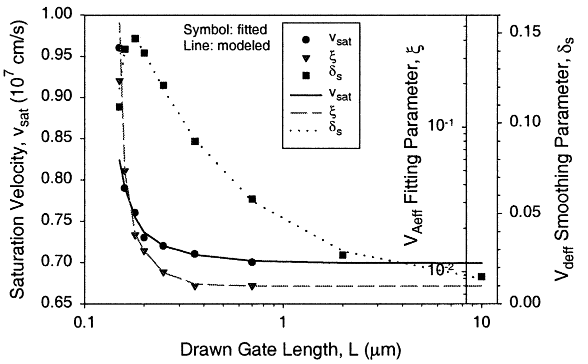

Figure 6: Individually fitted (*symbols*) (on I_{ds}–V_{ds} at V_{gs} = 1.8 V, V_{bs} = 0) and empirically modeled (*lines*) (using data L = 0.16~10 μm) saturation velocity (v_{sat}, ○), CLM (ξ, ▽) and V_{deff} smoothing (δ_s, □) parameters. Model extrapolation for L = 0.15-μm is used in prediction in Figs. 1,2,3(*c*).

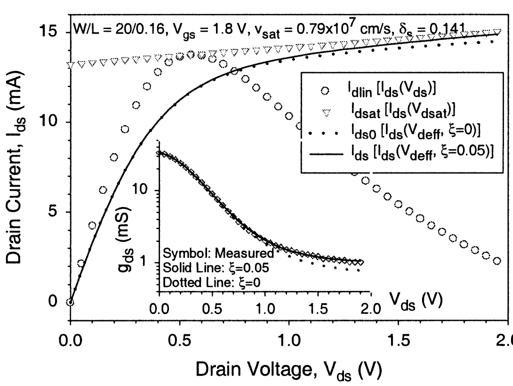

Figure 7: Modeled I_{ds}–V_{ds} characteristics using (1)–(3) with different components (using V_{ds}, V_{dsat}, or V_{deff}), showing the smooth transition from linear to saturation mode for both I_{ds} and g_{ds} (inset, dotted line: without CLM) with v_{sat} and ξ optimized for I_{ds} and g_{ds}, respectively, and δ_s based on g_{ds}'' data.

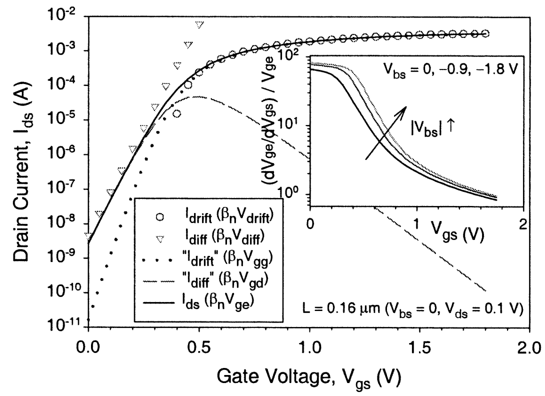

Figure 8: Modeled I_{ds}–V_{gs} characteristics using (1)–(3) with different components (using V_{drift}, V_{diff}, V_{gg}, V_{gd}, and V_{ge}), showing the smooth transition from strong inversion to subthreshold, which is built in for <u>all</u> length and bias with a <u>single</u> V_{off}. The inset shows the smooth derivatives, which supports the model results in Figs. 2,3 (◇) and Fig. 9.

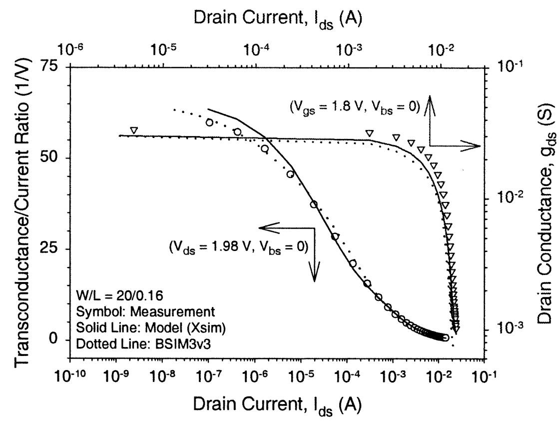

Figure 9: Measured (*symbols*) and modeled (Xsim: *solid lines*, BSIM: *dotted lines*) g_m/I_{ds} and log(g_{ds}) versus log(I_{ds}) characteristics, showing the smooth transitions in strong/weak-inversion and linear/saturation regions.

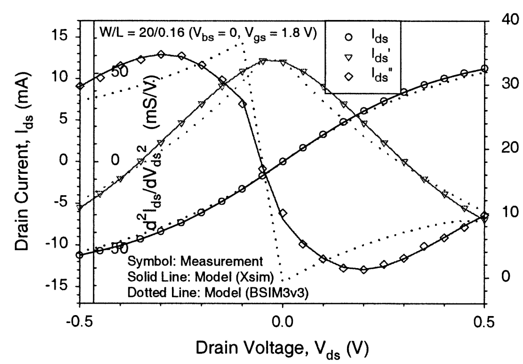

Figure 10: Measured (*symbols*) and modeled (Xsim: *solid lines*, BSIM: *dotted lines*) symmetry test around V_{ds} = 0, showing Xsim accuracy in higher-order derivatives (similar behavior is also observed in true Gummel test at various V_{gbo}, which is uncommon for source-referenced models).